One-to-one coupling of glacial climate variability in Greenland and Antarctica

EPICA Community Members*

Precise knowledge of the phase relationship between climate changes in the two hemispheres is a key for understanding the Earth's climate dynamics. For the last glacial period, ice core studies[1,2] have revealed strong coupling of the largest millennial-scale warm events in Antarctica with the longest Dansgaard–Oeschger events in Greenland[3–5] through the Atlantic meridional overturning circulation[6–8]. It has been unclear, however, whether the shorter Dansgaard–Oeschger events have counterparts in the shorter and less prominent Antarctic temperature variations, and whether these events are linked by the same mechanism. Here we present a glacial climate record derived from an ice core from Dronning Maud Land, Antarctica, which represents South Atlantic climate at a resolution comparable with the Greenland ice core records. After methane synchronization with an ice core from North Greenland[9], the oxygen isotope record from the Dronning Maud Land ice core shows a one-to-one coupling between all Antarctic warm events and Greenland Dansgaard–Oeschger events by the bipolar seesaw[6]. The amplitude of the Antarctic warm events is found to be linearly dependent on the duration of the concurrent stadial in the North, suggesting that they all result from a similar reduction in the meridional overturning circulation.

The glacial climate in the North Atlantic region is characterized by rapid shifts from cold stadial to warmer interstadial conditions[3,4,9]. Greenland temperatures during these Dansgaard–Oeschger (D–O) events rise by 8–16 °C (refs 10, 11) within a few decades followed by a less rapid temperature decline back to stadial conditions. In contrast, glacial climate in the circum-Antarctic region exhibits slower millennial changes with smaller temperature amplitudes of only 1–3 °C (refs 1, 12, 13). After synchronization of Greenland and Antarctic ice core records[1,2] using the global atmospheric change in CH_4 concentrations, a conspicuous phase relationship between the largest Antarctic warmings (A1–A7; ref. 1) and the longest D–O events was observed with the south warming during the stadial conditions in the north, and starting to cool as soon as the D–O warming set in. This bipolar seesaw pattern was explained by changes in the heat and freshwater flux connected to the Atlantic Meridional Overturning Circulation (MOC), where a stronger MOC leads to increased drainage of heat from the Southern Ocean heat reservoir[6,7].

In principle, an interhemispheric climate coupling by the bipolar seesaw should also apply for all the short D–O events. However, to what extent this concept is also able to explain the higher-frequency climate variability in Antarctic ice cores remained unclear (as discussed for example, in ref. 14 and references therein). Here we report

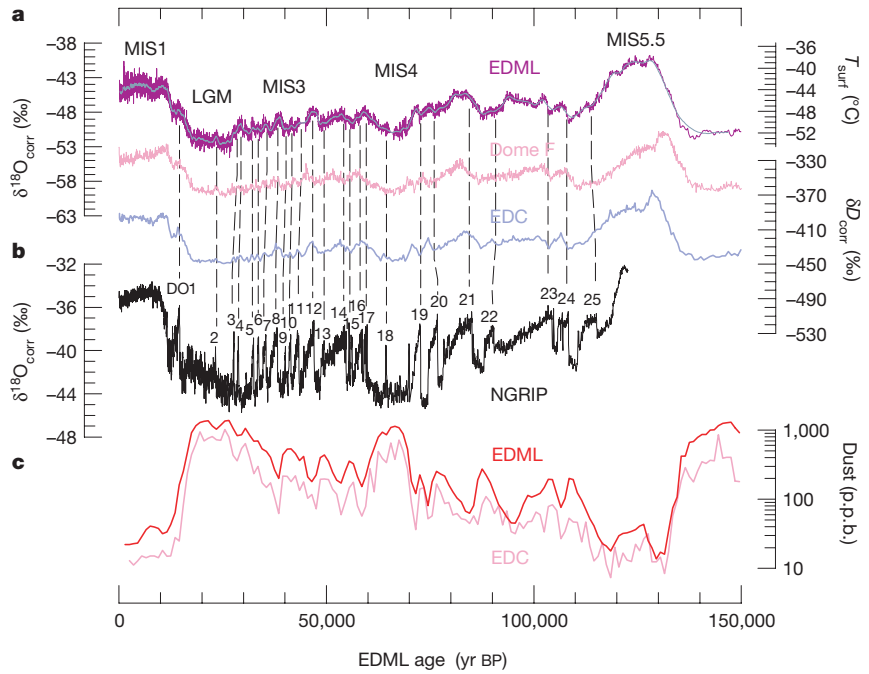

Figure 1 | Antarctic stable isotope records show synchronous millennial variations during the last glacial, whereas rapid variations are encountered in Greenland. **a**, EDML $\delta^{18}O$ record (purple, 0.5-m resolution; grey, 15-m running mean) after sea level and upstream correction (see Supplementary Information) over the past 150 kyr. The record shows features similar to those of the EDC[12] (blue) and the Dome F[13] (pink) isotope records but with more fine structure during MIS3 and MIS4. We note that EDML and EDC are plotted on the new common EDC3 timescale (see Supplementary Information) while Dome F is plotted on its individual timescale. The temperature axis on the right side indicates approximate surface temperatures at EDML as derived from the spatial $\delta^{18}O$/temperature gradient (see Supplementary Information). **b**, $\delta^{18}O$ record of the NGRIP ice core (grey)[9]. **c**, Mineral dust records of the EDML (red) and EDC[12] (pink) ice cores at 1,000-yr resolution; these dust records were used for synchronization of the cores.

*A full list of authors and their affiliations appears at the end of the paper.

on the climate record over the last glacial cycle from a new ice core drilled within the European Project for Ice Coring in Antarctica (EPICA) in the interior of Dronning Maud Land, hence denoted EDML, at 75° S, 0° E, 2,892 m.a.s.l. (metres above sea level), with a recent accumulation rate of 6.4 cm water equivalent (w.e.) per year[15]. This site was chosen to complement the long EPICA Dome C (EDC, 75° S, 123° E, 3,233 m.a.s.l., 2.5 cm w.e. yr^{-1}) record[12], because EDML is the first deep ice core in the Atlantic sector of the Southern Ocean region[16] and thus located near the southern end of the bipolar seesaw. The snow accumulation at EDML is two to three times higher than at other deep drilling sites on the East Antarctic plateau, so higher-resolution atmosphere and climate records can be obtained for the last glacial period, making the EDML core especially suitable for studying decadal-to-millennial climate variations in Antarctica.

In Fig. 1 the EDML $\delta^{18}O$ record as proxy for local temperature on the ice sheet is shown in 0.5-m resolution (equivalent to 15–30 yr during the marine isotope stage MIS3 and 100–150 yr during MIS5) after correction for upstream and glacial–interglacial ice sheet altitude effects (see Supplementary Information). The overall pattern closely resembles that recorded in most Antarctic ice cores previously covering this time period[12,13,17]. Also, very similar dust profiles (Fig. 1) are encountered at EDML and EDC, related to parallel changes in climate conditions in the Patagonian dust source region common to both cores[18]. Despite the high correlation of the EDML $\delta^{18}O$ and the EDC δD record over the last 150,000 yr ($r^2 = 0.94$ for 250-yr averages) some distinct differences exist. In the penultimate warm period (MIS5.5) the EDML $\delta^{18}O$ record indicates temperatures about 4–5 °C higher than those of the Holocene, in line with other ice cores from the East Antarctic plateau[12,13,17]. However, $\delta^{18}O$ at EDML exhibits persistently higher $\delta^{18}O$ values over the entire duration of MIS5.5 while other ice cores on the East Antarctic plateau show a substantial drop after an initial climate optimum[12,13]. We note that this difference is not due to the altitude corrections applied to the EDML $\delta^{18}O$ record (see Supplementary Information), because a similar temporal evolution during MIS5.5 is also seen in the uncorrected data. Instead, a smaller cooling at EDML in the course of MIS5.5 compared to EDC and Dome Fuji is consistent with marine sediment records from the Atlantic sector of the Southern Ocean revealing persistently warmer summer sea surface temperatures and a reduced winter sea ice cover throughout MIS5.5 (ref. 19). This suggests that there were regional differences in temperature and sea ice evolution during this period for the Atlantic and Indian Ocean sector.

The most outstanding feature of the high-resolution EDML record is the pronounced millennial variability during the glacial. As indicated by the dashed lines in Fig. 1 each of the warming episodes in Antarctica can be related to a corresponding D–O event, but only synchronization of the age scales allows us to assign them unambiguously and to pinpoint the phase relationship between climate changes in Greenland and Antarctica. To do this, the EDML core has been synchronized (see Supplementary Information) to the layer counted NGRIP ice core[20,21] over MIS3, using high-resolution CH_4 profiles over the last 55 kyr from the NGRIP, GRIP and GISP2 ice cores[1,11]. The synchronized $\delta^{18}O$ records are shown in Fig. 2. Also plotted is the CH_4 synchronized $\delta^{18}O$ record from the Byrd ice core[1] and new high-resolution δD data from EDC[22] which closely resemble the temperature variability found at EDML during MIS3 and support an Antarctic-wide interpretation of these fluctuations. The higher glacial snow accumulation at EDML (~3 cm w.e. yr^{-1}) compared to that at EDC, Dome Fuji or Vostok (~1.4 cm w.e. yr^{-1}) implies a CH_4 synchronization two to three times better than at those sites. The synchronization uncertainty for MIS3 ranges from 400 to 800 yr for all events in the EDML record, making the synchronization error for EDML always much smaller than the duration of the events themselves.

This is important, because this allows an unequivocal one-to-one assignment not only of the well-known large warm events in Antarctica (A1, A2 and so on) but of each single isotope maximum indicated in Fig. 2 with a corresponding D–O event in the north. Although the exact timing of the temperature maxima relative to the stadial/interstadial transitions cannot be discerned more precisely than the synchronization error, it is evident that each Antarctic warming starts significantly before the respective D–O event. In addition, a synchronization of the stable water isotope records of the GRIP and EDC ice cores using the ^{10}Be production anomaly around 41,000 yr BP, which constrains the in-phase relationship of the onset of D–O 10 and the respective Antarctic δD maximum to better than 200 yr (ref. 23), supports our CH_4 match. Accordingly, we suggest a new Antarctic Isotope Maximum (AIM) nomenclature in Fig. 2

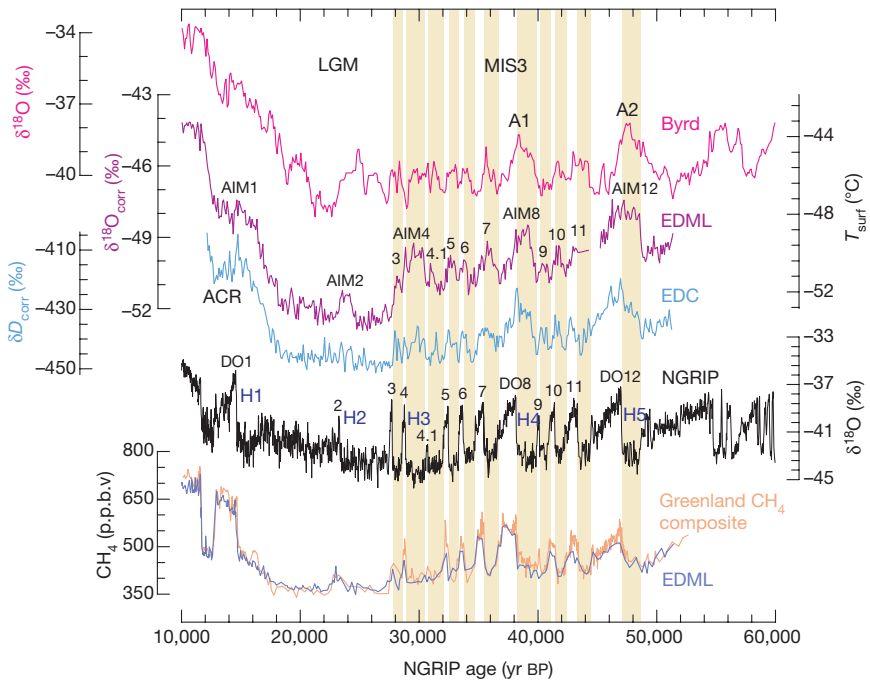

Figure 2 | Methane synchronization of the EDML and the NGRIP records reveals a one-to-one assignment of each Antarctic warming with a corresponding stadial in Greenland. Displayed are 100-yr averages during MIS3 in the EDML, EDC[26] and Byrd[1] ice core for the time interval 10–60 kyr BP in comparison with the NGRIP $\delta^{18}O$ record from Northern Greenland[9]. All records are CH_4 synchronized and given on the new GICC05 age scale for the NGRIP ice core, which has been derived by counting annual layers down to 41 kyr and by a flow model for older ages[9,21]. Yellow bars indicate the Greenland stadial periods that we relate to respective Antarctic temperature increases. The approximate timing of Heinrich layers in North Atlantic sediments is indicated as well[27]. The *y* axis on the right side indicates approximate temperature changes at EDML based on the modern spatial gradient between $\delta^{18}O$ and temperature.

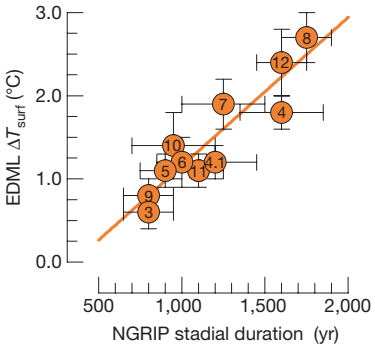

Figure 3 | Amplitudes of Antarctic warmings show a linear relationship ($r^2 = 0.85$) with the duration of the accompanying stadial in Greenland during MIS3. The amplitude was determined from the Antarctic $\delta^{18}O$ maximum to the preceding minimum of each event; the stadial duration is defined by the interval between the midpoint of the stepwise temperature change at the start and end of a stadial on the extended GICC05 age scale[9,21]. Error bars reflect the estimated uncertainty in the definition of the maxima and minima in $\delta^{18}O$ at EDML and in the duration of the concurrent stadial period. Numbers indicate the corresponding AIMs and D–O events.

which reflects the connection of southern warming to reduced oceanic heat transport into the North Atlantic during stadials. The timing and duration of the AIMs relative to D–O events is also indirectly supported by the comparison of changes in deep-water masses linked to Antarctic Bottom Water formation and Atlantic surface water changes, as archived in sediment records offshore of Portugal[24].

Most striking is the varying amplitude of the AIMs, which is linearly dependent on the duration of stadials in the north, as shown in Fig. 3. The only significant deviation from this linear relationship during MIS3 is AIM4, in which the error in the stadial duration estimate is quite large. We conclude that the duration of a reduced MOC—and, hence, the duration of the warming period in the Southern Ocean—determines the amount of heat accumulated in the Southern Ocean heat reservoir, strongly supporting the general applicability of the thermal bipolar seesaw[6] concept within the range of stadial events encountered during MIS3. We note that for longer cessations of the MOC a new equilibrium temperature in the Southern Ocean would be reached and the warming would eventually have to cease. This linear relationship also implies that the Antarctic warming rate—and thus the heat flux from the Southern Ocean to the Atlantic—is similar for all warming events during MIS3. If we assume the same spatial configuration of the overturning cell for cold intervals in MIS3, this would suggest that the strength of the MOC is approximately constant for all stadials, challenging the notion of different overturning rates[25] for stadials in which massive iceberg discharges into the North Atlantic (the so-called Heinrich events in Fig. 2: H1–H5) occurred compared to stadials without Heinrich events. Note however, that the stadials before D–O 8 and D–O 12 in which Heinrich events occurred were the longest and the related Antarctic warmings the largest. This may be due to the longer time needed to mix away the large freshwater anomalies during Heinrich events. There is, however, a less clear relationship for other Heinrich events. Comparison of the millennial climate variability during MIS3 at EDML and EDC shows no significant difference in the amplitude of the isotopic change in the Atlantic and Indian Ocean sectors of the Southern Ocean. This implies a uniform ocean heat reservoir controlling temperature changes at both sites and reflects the rapid mixing of the Southern Ocean by the Antarctic Circumpolar Current.

In the EDML $\delta^{18}O$ record a major warm event (AIM2, connected to D–O 2) is seen during the Last Glacial Maximum, which cannot be clearly identified in the EDC core but is present in the Dome F record (Fig. 1). AIM2 also shows a decrease in high-resolution mineral dust concentrations at EDC, as do all the other AIMs[26]. We therefore conclude that AIM2 is a warm event comparable to the other AIMs in MIS3 but is not sufficiently resolved in the EDC record owing to its lower accumulation. The corresponding D–O 2 event in the North Atlantic is preceded by the longest cold period in the NGRIP record (Fig. 2) and accordingly, a higher temperature amplitude of AIM2 is to be expected if the same bipolar seesaw concept holds as for D–O events during MIS3. However, sea level and temperature conditions were significantly different during the Last Glacial Maximum, potentially affecting the spatial configuration and strength of the overturning cell in the North Atlantic. The fact that AIM2 is only 2,000 yr long suggests that the strength of the MOC was not significantly reduced for the entire cold period in the North, but collapsed only about 1,000 yr before D–O 2, which would be in line with significant iceberg discharge depositing ice-rafted debris in the North Atlantic during H2 (ref. 27).

In summary, a strong interhemispheric coupling of all bipolar climate variations during MIS3 via the MOC is supported by the new high-resolution $\delta^{18}O$ record from EDML indicating that Antarctic warming rates and potentially also overturning rates have been similar for all events in MIS3. The question of what triggers the switch from stadial to interstadial conditions remains. Transitions in the strength of the MOC and its effect on the Atlantic Southern Ocean heat exchange are simulated in response to changes in the North Atlantic freshwater balance[7,8]; however, the origin of such variations in freshwater input are still not ascertained for all individual D–O events. In addition, large iceberg discharge from the Laurentide ice sheet does not systematically coincide with either the onset or the end of stadials[27,28]. Recently, the potential role of a change in Southern Ocean sea-ice cover for reinstalling a stronger MOC has been identified for the onset of the Bølling/Allerød warming[29,30]. The intrinsic feedback of a reduced sea-ice cover in the Southern Ocean during AIMs, followed by a delayed onset of deep-water formation in the North, could potentially explain the interhemispheric climate coupling seen in our records during MIS3.

Received 26 May; accepted 22 September 2006.

1. Blunier, T. & Brook, E. J. Timing of millennial-scale climate change in Antarctica and Greenland during the last glacial period. *Science* **291,** 109–112 (2001).
2. Blunier, T. *et al.* Asynchrony of Antarctic and Greenland climate change during the last glacial period. *Nature* **394,** 739–743 (1998).
3. Johnsen, S. J. *et al.* Irregular glacial interstadials recorded in a new Greenland ice core. *Nature* **359,** 311–313 (1992).
4. Bond, G. *et al.* Correlations between records from North Atlantic sediments and Greenland ice. *Nature* **365,** 143–147 (1993).
5. McManus, J. F., Oppo, D. W. & Cullen, J. L. A 0.5-million-year record of millennial climate variability in the North Atlantic. *Science* **283,** 971–975 (1999).
6. Stocker, T. F. & Johnsen, S. J. A minimum thermodynamic model of the bipolar seesaw. *Paleoceanography* **18,** art. no. 1087 (2003).
7. Knutti, R., Flückiger, J., Stocker, T. F. & Timmermann, A. Strong hemispheric coupling of glacial climate through freshwater discharge and ocean circulation. *Nature* **430,** 851–856 (2004).
8. Ganopolski, A. & Rahmstorf, S. Rapid changes of glacial climate simulated in a coupled climate model. *Nature* **409,** 153–158 (2001).
9. North Greenland Ice Core Project members. High resolution climate record of the northern hemisphere reaching into the last interglacial period. *Nature* **431,** 147–151 (2004).
10. Landais, A. *et al.* Quantification of rapid temperature change during DO event 12 and phasing with methane inferred from air isotopic measurements. *Earth Planet. Sci. Lett.* **225,** 221–232 (2004).
11. Huber, C. *et al.* Isotope calibrated Greenland temperature record over Marine Isotope Stage 3 and its relation to CH_4. *Earth Planet. Sci. Lett.* **245,** 504–519 (2006).
12. EPICA community members. Eight glacial cycles from an Antarctic ice core. *Nature* **429,** 623–628 (2004).
13. Watanabe, O. *et al.* Homogeneous climate variability across East Antarctica over the past three glacial cycles. *Nature* **422,** 509–512 (2003).
14. Roe, G. H. & Steig, E. J. Characterization of millennial-scale climate variability. *J. Clim.* **17,** 1929–1944 (2004).
15. Oerter, H. *et al.* Accumulation rates in Dronning Maud Land, Antarctica, as revealed by dielectric-profiling measurements of shallow firn cores. *Ann. Glaciol.* **30,** 27–34 (2000).
16. Reijmer, C. H., van den Broeke, M. R. & Scheele, M. P. Air parcel trajectories to five deep drilling locations on Antarctica, based on the ERA-15 data set. *J. Clim.* **15,** 1957–1968 (2002).

17. Petit, J. R. *et al.* Climate and atmospheric history of the past 420,000 years from the Vostok ice core, Antarctica. *Nature* **399,** 429–436 (1999).
18. Basile, I. *et al.* Patagonian origin of glacial dust deposited in East Antarctica (Vostok and Dome C) during glacial stages 2, 4 and 6. *Earth Planet. Sci. Lett.* **146,** 573–589 (1997).
19. Bianchi, C. & Gersonde, R. The Southern Ocean surface between Marine Isotope Stage 6 and 5d: Shape and timing of climate changes. *Palaeogeogr. Palaeoclimatol. Palaeoecol.* **187,** 151–177 (2002).
20. Rasmussen, S. O. *et al.* A new Greenland ice core chronology for the last glacial termination. *J. Geophys. Res.* **111,** D06102 (2006).
21. Andersen, K. K. *et al.* The Greenland ice core chronology 2005, 15–42 kyr. Part 1: Constructing the time scale. *Quat. Sci. Rev.* (in the press).
22. Stenni, B. *et al.* A late-glacial high-resolution site and source temperature record derived from the EPICA Dome C isotope records (East Antarctica). *Earth Planet. Sci. Lett.* **217,** 183–195 (2003).
23. Raisbeck, G., Yiou, F. & Jouzel, J. Cosmogenic ^{10}Be as a high resolution correlation tool for climate records. *Geochim. Cosmochim. Acta* **66,** abstr. A623 (2002).
24. Shackleton, N. J., Hall, M. A. & Vincent, E. Phase relationships between millennial-scale events 64,000–24,000 years ago. *Paleoceanography* **15,** 565–569 (2000).
25. Rahmstorf, S. Ocean circulation and climate during the past 120,000 years. *Nature* **419,** 207–214 (2002).
26. Röthlisberger, R. *et al.* Dust and sea-salt variability in central East Antarctica (Dome C) over the last 45 kyrs and its implications for southern high-latitude climate. *Geophys. Res. Lett.* **29,** article no. 1963 (2002).
27. Bond, G. & Lotti, R. Iceberg discharges into the North Atlantic on millennial time scales during the last glaciation. *Science* **267,** 1005–1010 (1995).
28. de Abreu, L., Shackleton, N. J., Joachim Schönfeld, J., Hall, M. & Chapman, M. Millennial-scale oceanic climate variability off the Western Iberian margin during the last two glacial periods. *Mar. Geol.* **196,** 1–20 (2003).
29. Knorr, G. & Lohmann, G. Southern Ocean origin for the resumption of Atlantic thermohaline circulation during deglaciation. *Nature* **424,** 532–536 (2003).
30. Stocker, T. F. & Wright, D. G. Rapid transitions of the ocean's deep circulation induced by changes in surface water fluxes. *Nature* **351,** 729–732 (1991).

Supplementary Information is linked to the online version of the paper at www.nature.com/nature.

Acknowledgements This work is a contribution to the European Project for Ice Coring in Antarctica (EPICA), a joint European Science Foundation/European Commission scientific programme, funded by the EU (EPICA-MIS) and by national contributions from Belgium, Denmark, France, Germany, Italy, the Netherlands, Norway, Sweden, Switzerland and the UK. The main logistic support was provided by IPEV and PNRA (at Dome C) and AWI (at Dronning Maud Land).

Author Information Reprints and permissions information is available at www.nature.com/reprints. The authors declare no competing financial interests. Correspondence and requests for materials should be addressed to H. F. (hufischer@awi-bremerhaven.de).

EPICA Community Members (listed in alphabetical order): C. Barbante[1,2], J.-M. Barnola[3], S. Becagli[4], J. Beer[5], M. Bigler[6,7], C. Boutron[3], T. Blunier[6], E. Castellano[4], O. Cattani[8], J. Chappellaz[3], D. Dahl-Jensen[7], M. Debret[3], B. Delmonte[9], D. Dick[10], S. Falourd[8], S. Faria[10,11], U. Federer[6], H. Fischer[10], J. Freitag[10], A. Frenzel[10], D. Fritzsche[12], F. Fundel[10], P. Gabrielli[2,3], V. Gaspari[1], R. Gersonde[10], W. Graf[13], D. Grigoriev[14], I. Hamann[10], M. Hansson[15], G. Hoffmann[8], M. A. Hutterli[6,16], P. Huybrechts[10,17], E. Isaksson[18], S. Johnsen[7], J. Jouzel[8], M. Kaczmarska[18], T. Karlin[15], P. Kaufmann[6], S. Kipfstuhl[10], M. Kohno[10], F. Lambert[6], Anja Lambrecht[10], Astrid Lambrecht[10], A. Landais[8], G. Lawer[10], M. Leuenberger[6], G. Littot[16], L. Loulergue[3], D. Lüthi[6], V. Maggi[9], F. Marino[9], V. Masson-Delmotte[8], H. Meyer[12], H. Miller[10], R. Mulvaney[16], B. Narcisi[19], J. Oerlemans[20], H. Oerter[10], F. Parrenin[3], J.-R. Petit[3], G. Raisbeck[21], D. Raynaud[3], R. Röthlisberger[16], U. Ruth[10], O. Rybak[10], M. Severi[4], J. Schmitt[10], J. Schwander[6], U. Siegenthaler[6], M.-L. Siggaard-Andersen[7], R. Spahni[6], J. P. Steffensen[7], B. Stenni[22], T. F. Stocker[6], J.-L. Tison[23], R. Traversi[4], R. Udisti[4], F. Valero-Delgado[10], M. R. van den Broeke[20], R. S. W. van de Wal[20], D. Wagenbach[24], A. Wegner[10], K. Weiler[6], F. Wilhelms[10], J.-G. Winther[18] & E. Wolff[16]

[1]Department of Environmental Sciences, University Ca' Foscari of Venice, [2]Institute for the Dynamics of Environmental Processes-CNR, Dorsoduro 2137, 30123 Venice, Italy. [3]Laboratoire de Glaciologie et Géophysique de l'Environnement (LGGE), CNRS-UJF, BP96 38402 Saint-Martin-d'Hères cedex, France. [4]Department of Chemistry, University of Florence, Via della Lastruccia 3, 50019 Sesto Fiorentino, Florence, Italy. [5]EAWAG, PO Box 611, 8600 Dübendorf, Switzerland. [6]Climate and Environmental Physics, Physics Institute, University of Bern, Sidlerstrasse 5, 3012 Bern, Switzerland. [7]Niels Bohr Institute, University of Copenhagen, Juliane Maries Vej 30, 2100 Copenhagen OE, Denmark. [8]Laboratoire des Sciences du Climat et de l'Environnement (LSCE/IPSL), CEA-CNRS-UVSQ, CE Saclay 91191, Gif sur Yvette, France. [9]Environmental Sciences Department, University of Milano Bicocca, Piazza della Scienza 1, 20126 Milano, Italy. [10]Alfred-Wegener-Institute for Polar and Marine Research, Columbusstrasse, D-27568 Bremerhaven, Germany. [11]Max Planck Institute for Mathematics in the Sciences, Inselstrasse 22, 04103 Leipzig, Germany. [12]Alfred Wegener Institute for Polar and Marine Research, Research Unit Potsdam, Telegrafenberg A 43, 14473 Potsdam, Germany. [13]GSF National Center for Environment and Health, Ingolstädter Landstrasse 1, 85764 Neuherberg, Germany. [14]University College London, Gower Street, London WC1E 6BT, UK. [15]Department of Physical Geography and Quaternary Geology, Stockholm University, 106 91 Stockholm, Sweden. [16]British Antarctic Survey, High Cross, Madingley Road, Cambridge CB3 0ET, UK. [17]Departement Geografie, Vrije Universiteit Brussel, Pleinlaan 2, 1050 Brussel, Belgium. [18]Norwegian Polar Institute, 9296 Tromsø, Norway. [19]ENEA, C. R. Casaccia, Via Anguillarese 301, 00060 Roma, Italy. [20]Utrecht University, Institute for Marine and Atmospheric Research, PO Box 80005, 3508 TA Utrecht, The Netherlands. [21]CSNSM/IN2P3/CNRS, Bat. 108, 91405 Orsay, France. [22]Department of Geological, Environmental and Marine Sciences, University of Trieste, Via E. Weiss 2, 34127 Trieste, Italy. [23]Département des Sciences de la Terre, Université Libre de Bruxelles, CP160/03, 1050 Brussels, Belgium. [24]Institute for Environmental Physics, University of Heidelberg, INF229, 69120 Heidelberg, Germany.